Acta Astronautica 209 (2023) 132–145

Contents lists available at ScienceDirect

Acta Astronautica

journal homepage: www.elsevier.com/locate/actaastro

Research paper

Optimization of orbit prediction strategies for GNSS satellites

Adrian Nowak *, Radosław Zajdel, Krzysztof Sośnica

Institute of Geodesy and Geoinformatics, Wrocław University of Environmental and Life Sciences, Grunwaldzka 53, Wrocław, 50-357, Poland

ARTICLE INFO

Keywords:
Orbit prediction
Force model
IGS
ILRS
GPS
Galileo
BeiDou

ABSTRACT

The ability to provide precise orbit prediction of Global Navigation Satellite System (GNSS) satellites is essential in a wide range of applications in space geodesy and Earth sciences, including near real-time and real-time GNSS applications, forming broadcast ephemerides, or supporting Satellite Laser Ranging stations in tracking. In this study, we evaluate the impact of orbit modeling strategies on the accuracy of orbit predictions on short (one-day), and long (multi-day) time scales, focusing on the selection of the optimal approach for handling solar radiation pressure (SRP), the effects of including pseudo-stochastic parameters, and the impact of the arc length used for the initial orbit fit. The analysis includes 300 days of predictions in 2021 and the satellites belonging to the GPS, Galileo, GLONASS, BeiDou-3, (BDS-3), and QZSS constellations. Fitting an initial 2-day orbit arc is the optimal solution for all analyzed navigation satellite constellations. When official satellite construction metadata are available, e.g. for Galileo/QZSS, the hybrid strategy of combining both empirical and physical models, i.e. the extended Empirical CODE Orbit Model (ECOM2) with box-wing models, leads to the best results. Otherwise, using only the ECOM2 is a better choice. Finally, the results indicate that for all navigation satellites, the introduction of pseudo-stochastic parameters deteriorates the prediction quality. When using the optimal prediction strategy, the 95th percentiles of the position errors after the 1st/4th/9th day of prediction are equal to 0.09/0.93/4.52, 0.22/1.71/9.69, 0.20/2.19/11.30, 0.23/1.80/9.39, 0.23/2.28/7.78m for GPS-IIF, Galileo FOC, GLONASS-M, BDS-3 CAST, and QZSS, respectively.

1. Introduction

The ability to provide accurate orbit prediction is essential for a wide range of applications in space geodesy and Earth sciences. Satellite orbit prediction is one of the main objectives underlying near-real-time and real-time Global Navigation Satellite System (GNSS) applications, atmospheric monitoring, and precise point positioning [1–4].

The interest in the orbit prediction length depends on the application. There is no arbitrary definition of what should be considered short or long-term orbit prediction. The near-real-time and real-time GNSS users who employ the satellite orbits for positioning are mostly interested in short-term predictions up to 24 h, which reflects the predicted part of the International GNSS Service (IGS, [5]) ultra-rapid orbit products [6]. Long-term orbit predictions can be critical for Satellite Laser Ranging (SLR) stations of the International Laser Ranging Service (ILRS) [7] to efficiently track satellites [8]. In navigation, predicted orbits can be used to reduce the Time to First Fix or to create broadcast ephemerides [9,10]. Although the broadcast ephemerides are updated on representative time scales down to 10 min for Galileo satellites to one day, the long-term GNSS orbit predictions should be of interest in case of the extended loss of contact between the control segment and a GNSS satellite, i.e. extended mode[1] [11].

In this article, by short-term prediction, we mean the first 24 h of the prediction. By long-term prediction, we mean the orbit extrapolated over one day and up to nine days, which is the longest prediction analyzed in this study.

Over the years, the prediction quality of navigation satellites has been analyzed in various studies. The studies by Choi et al. [12] and Geng et al. [13] discuss the impact of the fitting window (initial arc length) on the quality of orbit prediction for GNSS satellites. The results described in Choi et al. [12] suggest that the 40–45 h arc should be used for initial orbit fit to obtain the best orbit predictions. These results were verified in subsequent studies by Geng et al. [13] and narrowed down to a range of 42–45 h. Such solutions have been recommended by the authors for ultra-rapid orbits in the IGS Multi-GNSS Pilot Project (MGEX, [14]), i.e. integrated multi-GNSS orbit products. In Duan et al. [15], the authors compared the quality of ultra-rapid 6-h orbit predictions with real-time orbit estimates to serve real-time users. A comprehensive analysis of the quality of navigation satellite orbit prediction for four navigation systems, i.e., BeiDou-3 (BDS-3), Galileo,

* Corresponding author.
E-mail address: adrian.nowak@upwr.edu.pl (A. Nowak).

[1] https://www.gps.gov/technical/icwg/IS-GPS-200N.pdf.

https://doi.org/10.1016/j.actaastro.2023.04.040
Received 10 November 2022; Received in revised form 11 April 2023; Accepted 19 April 2023
Available online 24 April 2023

GLONASS, and QZSS in the long-term aspect was discussed by Najder and Sośnica [8].

This study aims to find the optimal strategy for providing GNSS satellite orbit prediction. For this purpose, we start by evaluating the impact of the orbit modeling strategy on the orbit prediction accuracy. In Section 3.1.1, we evaluate how the length of the initial orbit fit affects the quality of the orbit prediction, considering the periods from 1 to 5 days of initial fits. In Section 3.1.2, we focus on the selection of the best strategy in terms of modeling the SRP, including different test cases of incorporating the extended Empirical CODE Orbit Model (ECOM2) [16–18] and the a priori box-wing model [6,19,20]. Then, in Section 3.1.3, we test the impact of using pseudo-stochastic orbit parameters on the quality of GNSS orbit predictions [16]. In Section 3.2, we evaluate the quality of the short-term orbit prediction solutions as reflected in the potential user positioning accuracy using the orbital component of the Signal in Space Ranging Error (SISRE, [21]). Finally, in Sections 4 and 5, we provide conclusions and discussion.

This study investigates the optimal strategy for providing short- and long-term orbit predictions. Such studies have never been performed with the simultaneous use of five constellations of navigation satellites and the distinction between each group. The number of solutions performed for each solution provides a complete overview of the impact of the various factors studied on the quality of the orbit prediction.

2. Material and methods

Fig. 1 illustrates a block diagram of the data processing for the validation of orbit prediction as performed in this study using the Bernese GNSS Software [22]. The predicted orbits are compared with reference orbits, which are the final orbits provided by CODE[2] [23,24], as a part of the IGS MGEX initiative [14]. The ephemerides collected for the analyses cover the period from March 7, 2021, to December 31, 2021 (300 days), thus more than half of a draconitic year, which reflects the full range of elevations of the Sun above the orbital plane (β angles) [25]. Both predicted and reference orbits are provided in the form of discrete satellite positions and velocities given in the Earth-fixed reference frame. The continuous orbital arc is fitted into discrete satellite positions which enables direct comparison at given epochs. The processing details of the orbital arc fit are provided in Section 2.2. The root mean square of the fit of the orbital arc is at the millimeter level, thus we consider it fully sufficient for the purpose of this study.

2.1. Dataset

Currently, there are four operational GNSS — the American GPS, Russian GLONASS, European Galileo, and Chinese BDS-3. The four GNSS serve users with more than 120 satellites in Medium Earth Orbit (MEO). The performance of GNSS systems is complemented by Regional Navigation Satellite Systems such as the Japanese QZSS. Various systems or even satellite generations within the individual systems differ in terms of orbit characteristics, satellite construction, or the availability of detailed satellite metadata information. The technical details about the differences between the individual systems are provided by Langley et al. [26].

Table 1 summarizes the information about the analyzed satellites. In this study, we decided to focus on the set of navigation satellites, which are the best representatives of their groups (Table 1). The groups are specified mainly based on the systems, orbit characteristics, and satellite generation/type. The degradation of target prediction quality over time for the satellites in each group was assumed to be equivalent.

Some groups of navigation satellites are not included in the analysis. The satellite in the Geostationary Earth Orbit (GEO) of the QZSS constellation, SVN J003, is not included in the prediction quality analysis because of the limited usefulness of GEO satellites in geodesy and Earth sciences. The 2nd generation of BeiDou satellites (BDS-2) is also excluded from the analysis, because of the limited usefulness of this system concerning the existence of global BDS-3.

[2] http://ftp.aiub.unibe.ch/CODE_MGEX/.

2.2. Orbit processing strategy

This section contains information about the strategies for orbit processing used in the analysis. An overview of the background models employed in the orbit propagator is summarized in Table 2. These, to a great extent, follow the recommendations from the International Earth Rotation and Reference Systems Service (IERS) Conventions 2010 [27]. Orbit fitting/extrapolating is conducted using the ORBGEN program in the Bernese GNSS Software [22].

The quality of the orbit prediction methodology is assessed based on the orbit differences between the reference orbit (CODE MGEX) and the predicted orbits. The orbit differences are calculated every 15 min and decomposed in the orbit reference frame, i.e., radial, along-track, and cross-track. Orbit comparison does not indicate the absolute orbit accuracy. However, when the high quality of one reference orbit is confirmed, the other can be validated to assess the impact of the force modeling used, e.g., the impact of the SRP modeling, which is the purpose of this study.

2.3. GNSS orbit modeling towards handling of non-gravitational forces

For the navigation satellites, the main orbit perturbations that can affect the orbit prediction quality are non-gravitational forces, such as direct SRP, and indirect solar radiation effects, including albedo and thermal effects. Given the high accuracy of models for the gravitational forces acting on a GNSS satellite, the lack of adequate predictability of non-gravitational forces acting on a satellite poses a technical and practical limit to short and mainly long-term predictions of GNSS satellite orbits [9]. In contrast to low-Earth orbiters, navigation satellites are not subject to substantial perturbations due to atmospheric drag, which causes the main limiting factor for orbit predictions of the latter [8]. The time-variable gravity field can also affect the prediction of GNSS orbits. However, at GNSS altitudes the dominating perturbation is associated with degree-2 gravity field coefficients. GPS satellites are in resonance with some coefficients of the Earth's gravity field but gravity field variations can also be absorbed by the empirical orbit parameters of the ECOM2 [34,35].

The main difficulties in providing accurate orbit predictions are: (1) the accumulation of the errors in all the background models considered in the orbit determination process, and (2) the dynamic variability of the perturbation forces, which have to be accounted for using a given set of parameters. One should also note that some propagation errors in numerical methods are related to discretization errors of the numerical integration scheme [36]. Moreover, Najder and Sośnica [8] point out that the prediction quality varies depending on the angle of the Sun's elevation above the orbital plane. Thus, at least half of the draconitic year should be taken into account to consider different orbit geometries and properly assess the prediction orbit quality.

Direct SRP is the main non-gravitational source of accelerations acting on navigation satellites. To evaluate its impact, different solutions based on the ECOM2 and the analytical a priori box-wing model are tested [37]. Simplified analytical models such as box-wing are not sufficient to compensate for all the changes in external conditions such as direct solar radiation, solar wind, or thermal effects. Therefore, without any empirical models, analytical models lead to the orbit modeling of a meter-level accuracy [37]. ECOM2 was proposed by Arnold et al. [18] to absorb the impact of the SRP acceleration on satellite solar panels and buses of different shapes:

$$\begin{cases} D(u) = D_0 + D_{2C}cos2\Delta u + D_{2S}sin2\Delta u \\ \qquad\qquad + D_{4C}cos4\Delta u + D_{4S}sin4\Delta u, \\ Y(u) = Y_0, \\ B(u) = B_0 + B_C cos\Delta u + B_S sin\Delta u, \end{cases} \tag{1}$$

Table 1
Analyzed satellites divided into groups. Bold font indicates the satellites selected for visualization. The dominant SVN-PRN assignment is given for the analysis period.

System	Type	Satellites		Orbit
		SVN numbers	PRN numbers	
GPS	GPS-IIR	G043,G045,G047,G051, G056,G059,**G061**	G13,G21,G22,G20, G16,G19,**G02**	MEO
	GPS-IIR-M	G048,**G050**,G052,G053, G055,G057,G058	G07,**G05**,G31,G17, G15,G29,G12	
	GPS-IIF	G062,G063,G064,G065, G066,G067,G068,G069, G070,G071,G072,**G073**	G25,G01,G30,G24, G27,G06,G09,G03, G32,G26,G08,**G10**	
	GPS-III	G074,G075,G076, **G077**,G078,G079	G04,G18,G23, **G14**,G11,G28	
Galileo	Galileo-1 IOV	E101,E102,**E103**	E11,E12,**E19**	MEO
	Galileo-2 FOC ecc.	**E201**,E202	**E18**,E14	
	Galileo-2 FOC	E203,E205,E206,E207, E208,E209,E210,E211, E212,E213,E214,E215, E216,E217,E218,E219, E220,E221,**E222**	E26,E24,E30,E07, E08,E09,E01,E02, E03,E04,E05,E21, E25,E27,E31,E36, E13,E15,**E33**	
GLONASS	GLONASS-M	R719,R720,R721,R730, R735,R736,R743,R744, R745,R747,R854,R851,**R852**	R20,R19,R13,R01, R22,R16,R08,R03, R07,R02,R18,R17,**R14**	MEO
	GLONASS-M+	R855,R856,R857, R858,**R859**,R860	R21,R05,R15, R12,**R04**,R24	
	GLONASS-K	**R802**,R805	**R09**,R11	
BeiDou	BDS-3 SECM	C203,C204,C207, **C208**,C212,C211, C216,C215	C27,C28,C29, **C30**,C25,C26, C34,C35	MEO
	BDS-3 CAST	C201,C202,**C206**, C205,C209,C210, C213,C214,C218,C219	C19,C20,**C21**, C22,C23,C24, C32,C33,C36,C37	
QZSS	IGSO	J001,**J002**,J004	J01,**J02**,J03	IGSO

Table 2
Description of the processing strategy and the background models.

Processing feature	Adopted processing strategy	
	Reference orbits	Predicted orbits
Navigation satellites considered	Galileo, GPS, GLONASS, BDS-3, QZSS (98 satellites)	
Time span	07.03.2021–31.12.2021	
A priori reference frame	IGb14 [28]	
Loading corrections	Ocean loading corrections: FES2004 [29]	
Earth orientation parameters	A priori polar motion and UT1-UTC from IERS C04 series aligned to ITRF2014 [30]	
Navigation Antenna Thrust	Yes	
Albedo reflectivity and emissivity	Yes	
Earth gravity potential	EGM2008 [31]	
Solid Earth tides	TIDE2000	
Planetary ephemeris file	DE421	
Sub-daily ERPs	IERS2010XY [27]	
Precession and Nutation model	IAU2006A [32,33]	
Time frame	GPS	
Earth potential max degree x order/ Ocean tides max degree x order	12 × 12/8 × 8	
Dynamical orbit parameters	New CODE model ECOM2 with 7 parameters [18]	Depending on the test case with different variants of using the new CODE model ECOM2 + a priori box-wing model for SRP (Section 3.1)
Pseudo-stochastic parameters	1 parameter in 3 directions: radial, along-track, cross-track, every 1 h after Beutler et al. [16]	Two options based on an interval of 6 and 12 h in the along-track, cross-track, radial directions, after Beutler et al. [16] (Section 3.1)

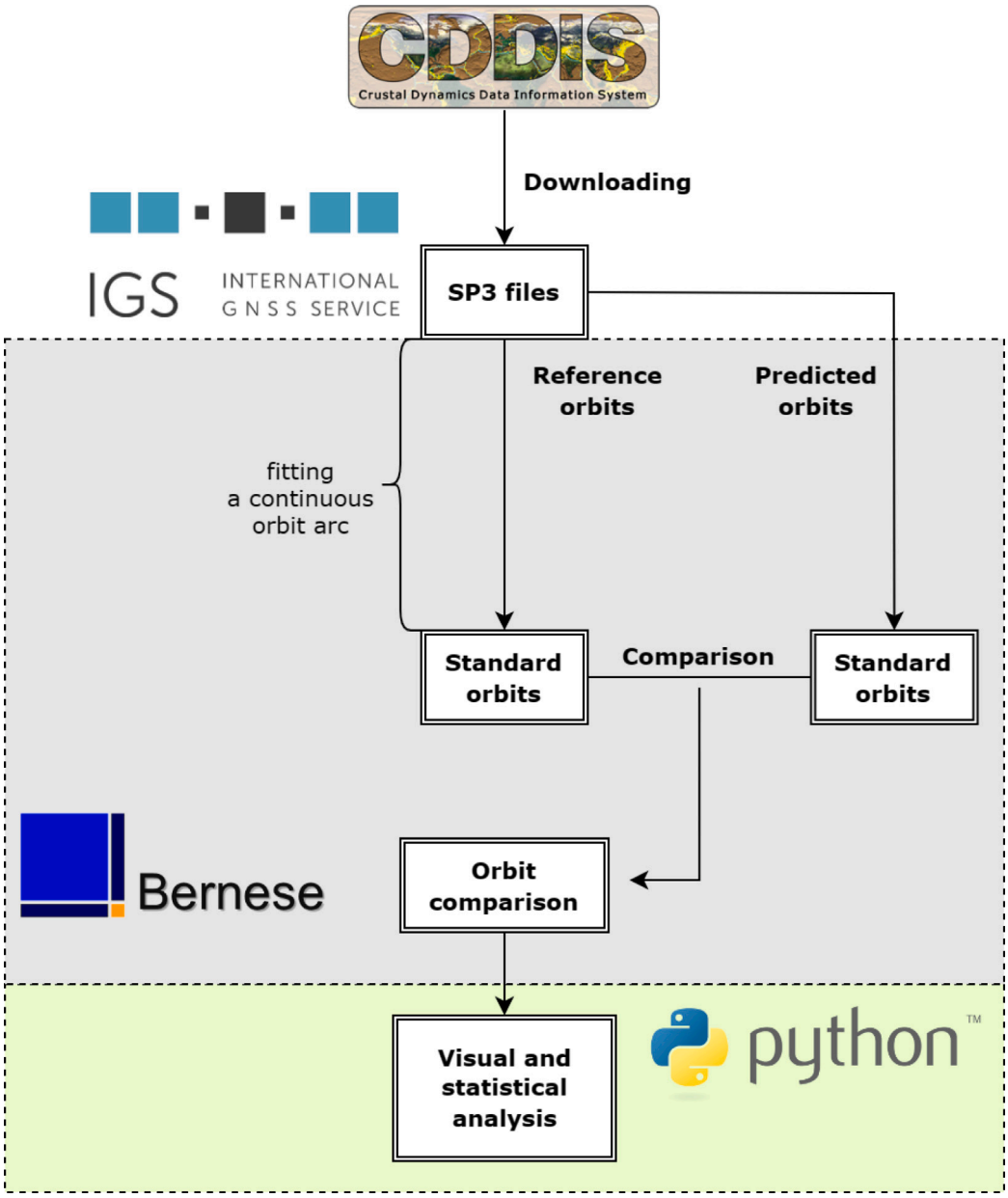

Fig. 1. Scheme of data processing.

where (u) is the satellite's argument of latitude, u_s is the argument of latitude of the Sun, and $\Delta u = u - u_s$ represents the argument of latitude with respect to the Sun.

Concerning the SRP modeling, eight solutions have been designed. The detailed characteristics along with the nomenclature of each solution are described in Table 3. These approaches are grouped into two main groups: the first involves the use of the ECOM2 (Eq. (1)) alone with a different number of estimated parameters: 3 (constant accelerations in DYB directions), where D is satellite-Sun direction, Y is aligned with the solar panel rotation axis, and B completes the right-handed orthogonal system being perpendicular to D and Y), 5 (additional sine and cosine once-per-revolution terms in B), 7 (additional sine and cosine twice-per-revolution terms in D) and 9 (additional sine and cosine fourfold-per-revolution terms in D) [18]. On the other hand, the second group is a combination of the first group and the use of an a priori box-wing model[3] [19,20,37–39]. In each solution, Earth albedo, infrared radiation, and transmitting antenna thrust are consistently considered (Table 2).

Table 3
List of empirical orbit parameters from ECOM2 and a priori box-wing models used in different solutions for orbit predictions.

Solution	Box-wing	Empirical orbit parameters (ECOM2)
E3	No	D_0, Y_0, B_0
E5	No	D_0, Y_0, B_0, B_S, B_C
E7	No	D_0, Y_0, B_0, B_S, B_C, D_{2C}, D_{2S}
E9	No	D_0, Y_0, B_0, B_S, B_C, D_{2C}, D_{2S}, D_{4C}, D_{4S}
B_E3	Yes	D_0, Y_0, B_0
B_E5	Yes	D_0, Y_0, B_0, B_S, B_C
B_E7	Yes	D_0, Y_0, B_0, B_S, B_C, D_{2C}, D_{2S}
B_E9	Yes	D_0, Y_0, B_0, B_S, B_C, D_{2C}, D_{2S}, D_{4C}, D_{4S}

Besides the dynamical orbit parameters related to SRP modeling, one can set up additional so-called pseudo-stochastic orbit parameters, which in standard precise orbit determination routines allow for partial

[3] http://acc.igs.org/repro3/PROPBOXW.f.

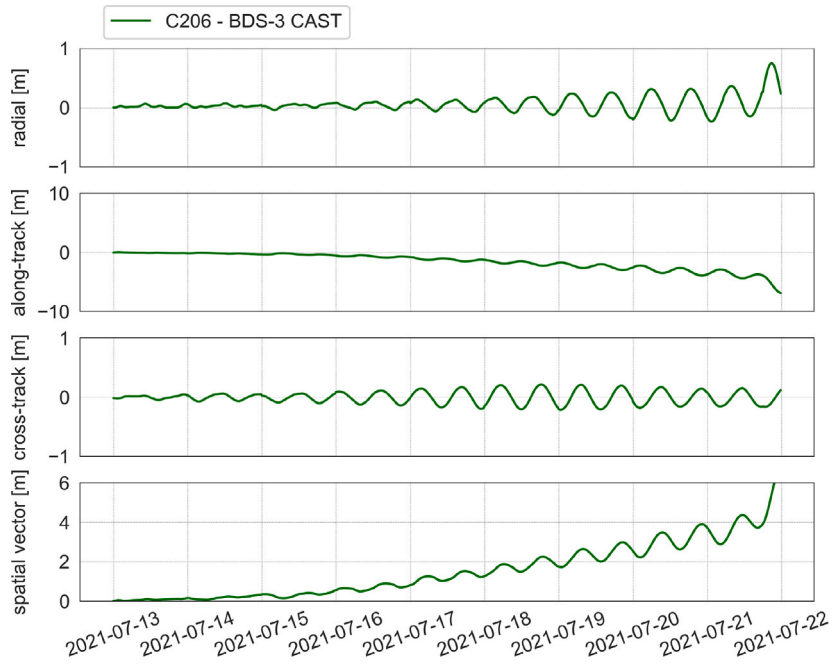

Fig. 2. Time series of the differences between the reference series (CODE MGEX final) and the nine-day orbit prediction for the BDS-3 MEO satellite. The y-axes for the along-track and 3D spatial vector are scaled 10 and 6 times, respectively.

reduction of the orbit modeling deficiencies [16]. These characterize instantaneous velocity changes at user-determined epochs and specified directions. When determining the orbits of GNSS satellites, one should keep in mind that the perturbing forces are not fully understood or the forces acting on the satellites change dynamically within the orbital arc. The pseudo-stochastic attribute is justified because usually a priori constraints (i.e., variances) are associated with these parameters. This procedure is comparable to 'stochastic' orbit modeling [40].

3. Results

In the next subsections, the results of the orbit comparison between reference and predicted orbits are discussed. Outliers are removed from the series at the pre-analysis stage using the interquartile range (IQR) method. Any observations exceeding 3.0 IQR below or above the median are considered outliers and removed from the analyses. In addition to the generated figures, statistics are calculated for the analyzed satellites in the form of medians and 95th percentiles for the individual components, i.e., radial (R), along-track (S), and cross-track (W), as well as for the 3D spatial vector.

A comparison of each component represented in the orbit reference frame shows substantial differences in the magnitude of prediction quality degradation over time. Fig. 2 shows the time series of the differences between the reference series and the nine-day orbit prediction for the BDS-3 MEO satellite. The analysis shows the sinusoidal, typically once-per-revolution nature of the differences between the predictions and precise satellite orbits. While the radial and cross-track directions remain within decimeter level at maximum, the errors in the along-track direction can reach a magnitude of several meters after a week of prediction. In general, we may observe that the prediction error in the along-track component constitutes from 97% to 99.9% of the total prediction error.

In terms of user positioning accuracy, the range error depends only on the line-of-sight component of the satellite orbit error. Based on Montenbruck et al. [21] the orbit-only contribution to the SISRE is expressed as:

$$SISRE_{orb} = \sqrt{w_R^2 \Delta r_R^2 + w_{A,C}^2 (\Delta r_A^2 + \Delta r_C^2)}, \quad (2)$$

where Δr_R, Δr_A, and Δr_C are the orbit errors in radial (R), along-track (A), and cross-track (C) directions, respectively. The elements w_R and $w_{A,C}$ are GNSS-dependent SISRE weight factors for the statistical contribution of R, A, and C errors to the line-of-sight ranging error. For the example of the Galileo satellites w_R and $w_{A,C}$ equal 0.984 and 0.124, respectively.

One should note, that the radial component constitutes a major factor that determines the positioning quality. On the other hand, prediction errors in the along-track direction are critical for SLR tracking, as they show up as time biases at the tracking stations when ranging to the satellite.

3.1. Optimizing the GNSS orbit prediction accuracy

This part of the study focuses on optimizing the orbit prediction solution strategy. Firstly, in Section 3.1.1, we assess how the length of the orbit fit affects the quality of the orbit prediction. Secondly, in Section 3.1.2, we focus on the selection of the best strategy regarding the modeling of SRP including various test cases of incorporating ECOM2 and a priori box-wing model. Finally, in Section 3.1.3, we test the impact of including so-called pseudo-stochastic parameters. Based on these comparisons, we determine the best methodology for each satellite group (see Table 1).

3.1.1. Impact of the initial orbital arc fit

The first analysis in the study concerns the selection of the optimal arc length of the initial orbit to fit. Four solutions are tested based on the arc lengths of 1, 2, 3, and 5 days. Figs. 3 and 4 show the degradation of prediction quality for the 1st and 4th prediction day, respectively. The figures on the vertical axis show the Root Mean Square (RMS) values for the 3D spatial vector. To have a complete overview, the analysis is performed for solutions based solely on the ECOM2 with 7 parameters and in a hybrid option with a box-wing model (solutions E7 and B_E7).

The statistics for all the solutions are shown in Table 4. The results indicate that the approach based on a one-day orbit arc to fit is the optimal solution only for a pair of Galileo satellites in an eccentric orbit. The results show that fitting a 2-day orbit arc is the optimal

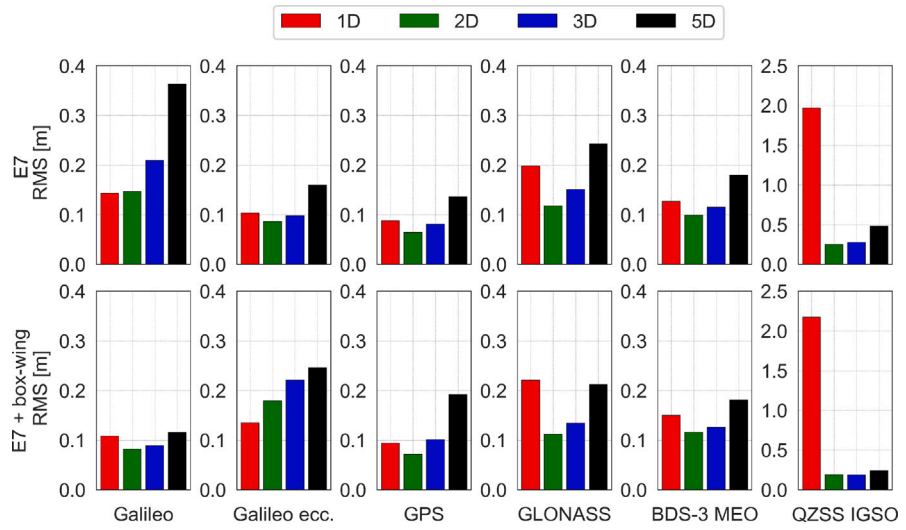

Fig. 3. Impact of the arc length of the initial orbit fit on the quality of the orbit prediction for different satellite types (columns) on the 1st prediction day. The first row shows the ECOM2-only solution, while the second row shows the hybrid ECOM2+box-wing solution. The *y*-axis for QZSS is scaled approximately 6.25 times.

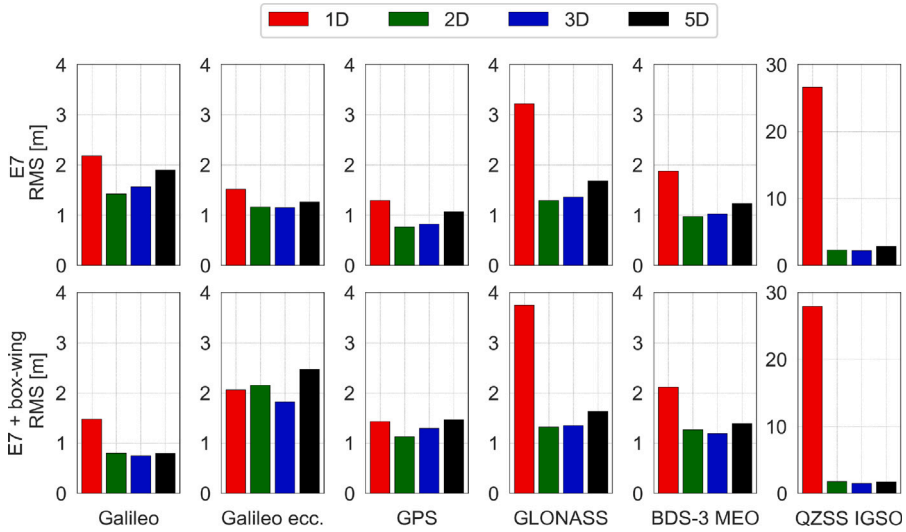

Fig. 4. Impact of the arc length of the initial orbit fit on the quality of the orbit prediction for different satellite types (columns) on the 4th prediction day. The first row shows the ECOM2-only solution, while the second row shows the hybrid ECOM2+box-wing solution. The *y*-axis for QZSS is scaled approximately 6.25 times.

and universal solution for almost all analyzed satellite groups. The 2-day solution is especially recommended for short-term prediction. The only exception is Galileo FOC satellites on highly eccentric orbit (ecc.) for which the 1-day initial orbit fit leads to the best results (Fig. 3). Further extension of the orbit arc length during the fitting deteriorates the solution in the vast majority of cases (Fig. 4). 2 days are 3 to 5 revolutions of MEO GNSS satellites or 2 revolutions of IGSO. This number of revolutions is sufficient to reliably determine ECOM2 parameters. Longer revolutions can average out more time-varying effects. Due to the above, the next analyses will only consider the case of the 2-day fit of the initial orbit.

3.1.2. *Impact of the SRP modeling*

Fig. 5 shows the long-term orbit prediction quality for the different processing strategies. The numerical details for the best solutions are given in Table 5 containing median and 95th percentile values for each processing strategy and satellite for the 4th day of prediction. For all the analyzed cases, using only three constant ECOM2 coefficients (E3 and B_E3) leads to the worst results (see Fig. 5).

The hybrid strategy of combining both empirical and physical models is beneficial for the quality of orbit prediction for the Galileo IOV, Galileo FOC, GLONASS-M and M+, BDS-3 CAST, and QZSS satellites. In addition, for two groups of GPS satellites, GPS-IIR-M and GPS-III, the hybrid solutions performed at approximately the same level as those based solely on ECOM2.

The recommended solution for both Galileo FOC and IOV satellites is a hybrid solution with five ECOM2 parameters (B_E5), however, increasing the number of ECOM2 parameters has no negative impact on the quality of the solution. As opposed to the other Galileo satellites, the ECOM2-only approach is recommended for the Galileo satellites on the highly eccentric orbit, which is reflected by the lowest median and 95% of the position error. For the Galileo FOC ecc. satellite, the best approach for SRP modeling is E7 and E9.

For GPS satellites, the ECOM2-only solutions are also beneficial compared to those based on the hybrid approach for SRP modeling, especially for the IIR, IIR-M, and IIF blocks. It should be noted that official information about the optical and geometrical properties of GPS satellites have never been publicly released. Therefore, the box-wing models of the GPS satellites are based on the long-term empirical fit of the coefficients [41].

Concerning GLONASS-M and M+ satellites, the best prediction results for orbits come from the strategy based on ECOM2 with the

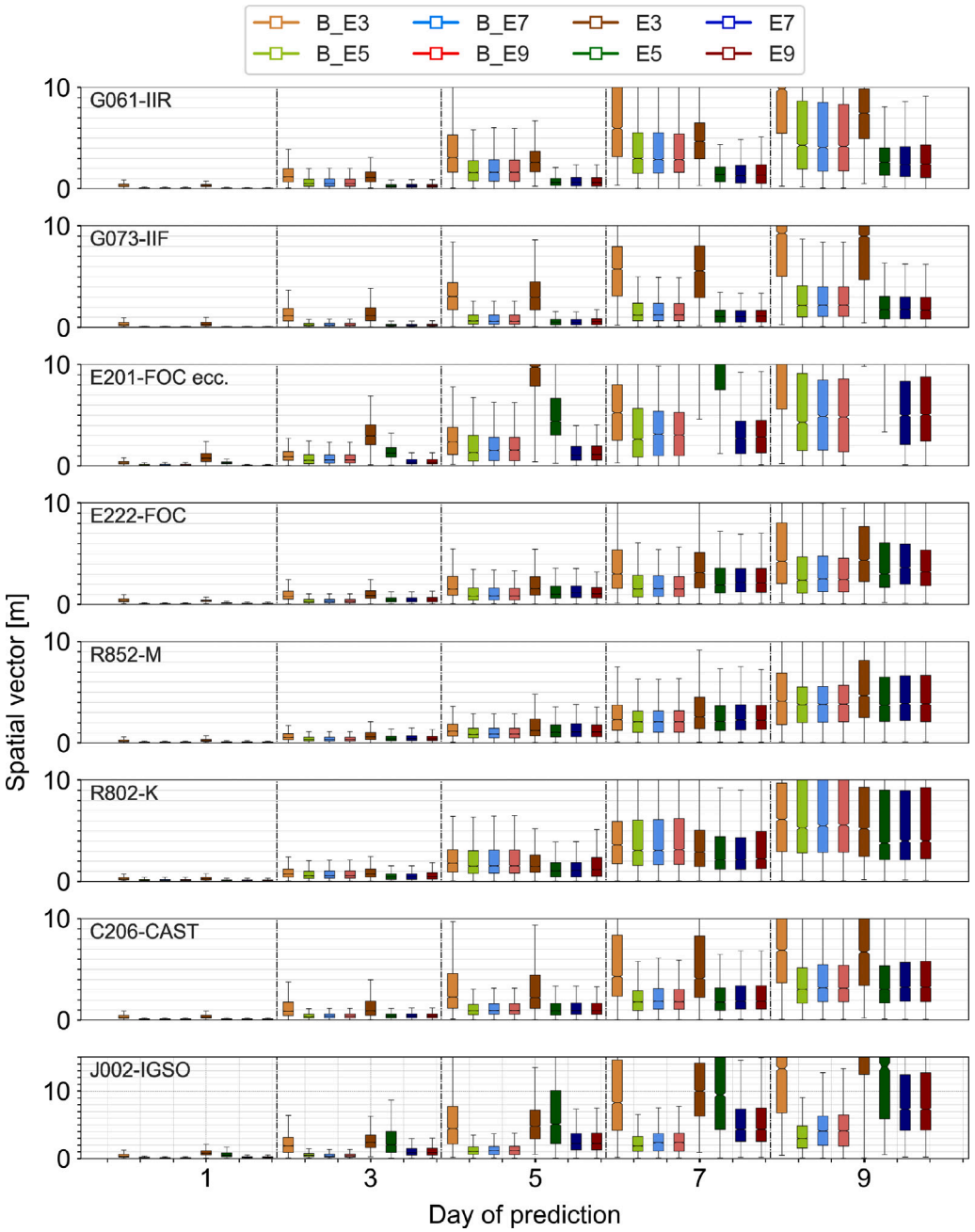

Fig. 5. Prediction quality degradation results over time for the spatial vector 3D and particular solutions shown in the form of box-whisker plots.

box-wing model. No significant differences are observed between the solutions B_E5, B_E7, and B_E9, which do not exceed 1 cm m with respect to the median position error on the 4th day of prediction. For GLONASS-M and M+ satellites, better results are obtained for the hybrid solution compared to GPS satellites. ECOM2 was originally designed for GPS, and even in the extended version [18], it works better with GPS than with the other GNSS constellations. For GLONASS, this is due to the elongated cylindrical shape of these groups of satellites. When ECOM2 does not work well, the box-wing model seems to improve the prediction solutions, which is not necessarily the case for GPS satellites. In the case of the GLONASS-K satellites, there is no effect of including the a priori box-wing model in the solution. On average, the prediction solutions for the hybrid models are worse than the ECOM2-based solutions by about 0.3 m on the 4th prediction day.

For the BDS-3 Shanghai Engineering Center for Microsatellites (SECM) group satellites, the E5 solution proved to be the best approach. It should be noted that the 95th percentile of the orbit error for the SECM satellites is about 0.5 m higher than for the BDS-3 China Academy of Space Technology (CAST) satellites. The differences can be attributed to differences in the design of the SECM and CAST satellites. The buses of the BDS-3 SECM satellites are extended in different directions than those of the BDS-3 CAST satellites. The Z-bus area with transmitter antennas is much larger than the X-bus area for SECM satellites, which is the opposite for CAST. In addition, the CAST satellites are slightly more cuboidal and their complex T-shape may give poor results using only the ECOM2. The small effect of using the box-wing model for BDS-3 satellites may be due to the incomplete official optical parameters provided by the China Satellite Navigation Office (CSNO) [39].

For the QZSS satellite, the most reliable QZSS orbit prediction results are provided by the strategy, in which the box-wing model is included. For QZSS, the impact of using the box-wing model is

Table 4
RMS values for the 1st and 4th day of prediction separated by satellite group and arc length of the initial orbit fitting. Bold font indicates values for the optimal solution, while the best result overall is given in bold green.

Type	Arc length	1st day of prediction [m]		4th day of prediction [m]	
		E7	B_E7	E7	B_E7
Galileo	1D	0.14	0.11	2.18	1.48
	2D	**0.15**	**0.08**	**1.42**	**0.80**
	3D	0.21	0.09	1.56	**0.74**
	5D	0.36	0.12	1.89	0.80
Galileo ecc.	1D	0.10	0.14	1.52	2.06
	2D	**0.09**	**0.18**	**1.16**	**2.15**
	3D	0.10	0.22	**1.15**	1.82
	5D	0.16	0.25	1.26	2.47
GPS	1D	0.09	0.09	1.29	1.43
	2D	**0.06**	**0.07**	**0.76**	**1.12**
	3D	0.08	0.10	0.82	1.30
	5D	0.14	0.19	1.07	1.47
GLONASS	1D	0.20	0.22	3.22	3.74
	2D	**0.12**	**0.11**	**1.29**	**1.32**
	3D	0.15	0.13	1.35	1.35
	5D	0.24	0.21	1.68	1.63
BDS-3 MEO	1D	0.13	0.15	1.87	2.11
	2D	**0.10**	**0.12**	**0.98**	**1.26**
	3D	0.12	0.13	1.02	1.19
	5D	0.18	0.18	1.24	1.39
QZSS IGSO	1D	1.97	2.17	26.63	27.90
	2D	**0.25**	**0.19**	**2.27**	**1.75**
	3D	0.28	**0.19**	2.16	**1.47**
	5D	0.48	0.24	2.85	1.72

Table 5
Median (50%) and 95th percentile (95%) values for each processing strategy and satellite for the 4th prediction day. The best result from the group is given in bold green. Bold font indicates solutions at a similar level of quality to the best solution.

Satellite	[m]	B_E5	B_E7	B_E9	E5	E7	E9
G061	50%	1.02	1.03	1.02	**0.39**	**0.42**	**0.39**
GPS-IIR	95%	4.21	3.86	3.54	**1.50**	**1.38**	**1.39**
G050	50%	**0.43**	**0.44**	**0.44**	**0.41**	**0.42**	**0.40**
GPS-IIR-M	95%	**1.21**	**1.23**	**1.24**	1.47	1.50	**1.33**
G073	50%	**0.39**	**0.39**	**0.39**	**0.33**	**0.32**	**0.35**
GPS-IIF	95%	1.54	1.57	1.70	**0.95**	**0.93**	**1.00**
G077	50%	**0.50**	**0.55**	**0.55**	**0.54**	**0.58**	**0.50**
GPS-III	95%	1.83	2.06	2.08	2.00	1.95	**1.65**
E103	50%	**0.51**	**0.52**	**0.52**	1.21	1.29	1.30
GAL-IOV	95%	**1.69**	**1.64**	**1.72**	3.05	3.03	2.88
E201	50%	0.82	0.94	0.94	2.43	**0.62**	**0.64**
GAL-FOC ecc.	95%	3.72	3.88	4.59	5.99	**2.24**	**2.36**
E222	50%	**0.51**	**0.52**	**0.53**	0.66	0.71	0.72
GAL-FOC	95%	**1.71**	**1.71**	1.89	2.23	1.89	1.80
R852	50%	**0.58**	**0.58**	**0.58**	0.67	0.71	0.69
GLO-M	95%	**2.29**	**2.25**	**2.19**	3.27	3.29	**2.28**
R859	50%	**0.73**	**0.74**	**0.74**	0.86	0.86	0.91
GLO-M+	95%	**2.24**	**2.31**	**2.30**	2.70	2.84	2.76
R802	50%	1.00	1.03	1.03	**0.70**	**0.71**	0.79
GLO-K	95%	4.25	4.25	4.24	**2.68**	**2.72**	2.99
C208	50%	0.57	0.59	0.58	**0.52**	**0.53**	0.57
BDS-3 SECM	95%	2.24	2.28	2.48	**1.36**	**1.38**	1.55
C206	50%	**0.58**	**0.61**	**0.60**	**0.59**	**0.61**	**0.59**
BDS-3 CAST	95%	**1.80**	**1.88**	**1.90**	**1.89**	**1.91**	**1.87**
J002	50%	**0.72**	**0.71**	**0.71**	3.29	1.42	1.44
QZSS-IGSO	95%	**2.28**	**2.32**	2.41	14.68	4.49	4.52

the largest among all the analyzed satellite groups, leading to the improvement at the level of 48% (from 4.49 to 2.32 m) concerning the 95th percentile of the orbit error comparing the E7 and B_E7 solutions.

Let us sum up the prediction error for the specified groups on the 4th day of prediction. For the groups of satellites where the ECOM2 used solely leads to the superior results, the 95th percentile of the prediction error equals 0.9, 1.4, 1.4, 1.6, 2.2, and 2.7 m for the GPS-IIF, BDS-3 SECM, GPS-IIR, GPS-III, Galileo FOC ecc., and GLONASS-K groups, respectively. On the other hand, there are groups for which the predictions of the orbits in the hybrid solution are more suitable than when using ECOM2 standalone. These are GPS IIR-M, Galileo IOV, Galileo FOC, BDS-3 CAST, GLONASS-M/M+, and QZSS with the 95th percentile of the prediction error at the level of 1.2, 1.6, 1.7, 1.8, 2.2, and 2.3 m, respectively.

Fig. 6 illustrates the calculated values of the median position error for the solution incorporating only ECOM2 with 7 parameters (y-axis) versus the values obtained for the corresponding hybrid solution with the box-wing model applied (x-axis). Each point represents one satellite from the navigation systems analyzed: GPS, Galileo, BDS-3, GLONASS, and QZSS, in blue, green, black, red, and orange, respectively. Points above the diagonal mean that the solution with the a priori box-wing model achieves lower values of the median position error for the 4th day of prediction than the empirical ECOM2; thus, using box-wing leads to the improvement of the orbit prediction quality. Conversely, for the satellites below the diagonal, a solution using only ECOM2 is the optimal approach over the analysis period.

For GLONASS and BDS-3 satellites, the differences between the two analyzed solutions do not exceed 0.2 m. Similar characteristics apply to most GPS satellites. The exceptions are the older satellites of the GPS IIR and IIR-M groups, for which the use of the empirical model alone is a superior approach. For the Galileo satellites from the IOV and FOC groups, the use of a box-wing model is a better approach compared to the solution based on only ECOM2. However, one should note that there are two clusters of green points. One of them is characterized by significantly lower errors for the E7 solution while having a similar level for the B_E7 solution. All of these satellites are located in the orbital plane A, which is characterized by higher maximum elevations of the Sun above the orbital plane (β) compared to the other two planes of the Galileo system [42]. Unlike the rest of the Galileo satellites, using only ECOM2 is superior for both Galileo FOC ecc. satellites. For the QZSS IGSO satellites, the hybrid solution is significantly better (more than two times) than when using ECOM2 standalone.

To sum up, there is a benefit of using the box-wing model for the systems, which have official detailed metadata provided by the system operators, i.e., the European GNSS Agency (GSA) for Galileo or the Japan Aerospace Exploration Agency (JAXA) for QZSS. On the other hand, there are at most minor impacts of using approximated, 'best guess', or simplified models, which provide no improvement. This group includes GPS, BDS-3, and GLONASS satellites.

The next part of the analysis focuses on optimizing the accuracy of the short-term prediction, i.e., the first 24 h. Fig. 7 illustrates the quality degradation in the first 24 h of prediction for the same satellites representing different groups (see Table 1). Table 6 collects the median and 95th percentile position error values for the best solutions in each group of satellites.

The results shown in Fig. 7 follow the conclusions of the long-term prediction quality analysis. For the Galileo FOC ecc. group of satellites, solutions based on ECOM2 with 7 and 9 parameters are the most stable and have the lowest errors in the first 24 h of the prediction. For the other two groups of Galileo satellites, IOV and FOC, unquestionably, the most suitable are hybrid solutions with a box-wing model.

For GPS satellites, the best in terms of quality solutions are those with a minimum of 7 empirical parameters. Similar to the long-term analysis for the GPS-IIR group, the best solutions are those using ECOM2 alone. Differences for individual solutions in the first 24 h of the prediction do not exceed a single centimeter. The best quality predictions, not exceeding 0.05 m after 24 h, of all the analyzed satellite groups were obtained for the GPS-IIF group.

For GLONASS-K and BDS-3 SECM, using only the ECOM2 gives better results. It should be noted that the differences are insignificant,

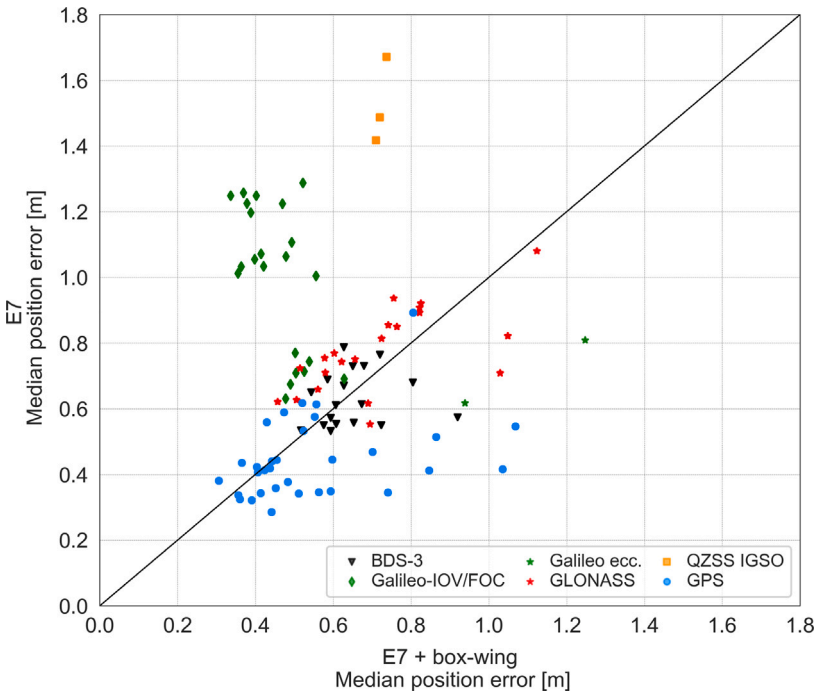

Fig. 6. Median position prediction error values for all satellites and the 4th day of the prediction. ECOM2 with 7 parameters (y-axis) versus ECOM2 with 7 parameters and box-wing model (x-axis). (For interpretation of the references to color in this figure legend, the reader is referred to the web version of this article.)

Table 6
Median (50%) and 95th percentile (95%) values for each processing strategy and satellite at 12/24 h of the prediction. Bold font indicates solutions at a similar level of quality to the best solution.

Satellite	[m]	B_E5	B_E7	B_E9	E5	E7	E9
G061	50%	0.06/0.09	0.06/0.09	0.06/0.09	0.05/0.08	**0.04/0.08**	**0.04/0.08**
GPS-IIR	95%	0.18/0.27	0.24/0.26	0.20/0.26	0.10/0.15	**0.08/0.14**	0.08/0.16
G050	50%	**0.04/0.06**	**0.04/0.06**	**0.04/0.06**	**0.05/0.06**	**0.04/0.06**	**0.04/0.06**
GPS-IIR-M	95%	**0.08/0.14**	**0.08/0.14**	**0.08/0.14**	0.10/0.16	0.10/0.14	**0.09/0.14**
G073	50%	**0.04/0.06**	**0.04/0.06**	**0.03/0.06**	**0.04/0.05**	**0.04/0.06**	**0.03/0.06**
GPS-IIF	95%	0.08/0.13	0.08/0.12	0.07/0.13	0.07/0.12	0.06/0.11	**0.06/0.09**
G077	50%	0.05/0.07	**0.04/0.07**	**0.04/0.06**	0.05/0.08	0.05/0.08	0.05/0.08
GPS-III	95%	0.11/0.15	**0.08/0.15**	0.10/0.15	0.12/0.17	0.12/0.16	0.10/0.15
E103	50%	**0.08/0.12**	**0.08/0.12**	**0.08/0.12**	0.12/0.22	0.12/0.22	0.12/0.21
GAL-IOV	95%	**0.16/0.28**	**0.18/0.28**	**0.16/0.28**	0.21/0.45	0.20/0.41	0.18/0.40
E201	50%	0.07/0.15	0.06/0.15	0.07/0.15	0.23/0.39	**0.04/0.07**	**0.04/0.07**
GAL-FOC ecc.	95%	0.38/0.43	0.37/0.40	0.38/0.43	0.43/0.65	**0.11/0.20**	**0.11/0.20**
E222	50%	**0.04/0.08**	**0.04/0.08**	**0.04/0.08**	0.11/0.15	0.06/0.13	0.06/0.12
GAL-FOC	95%	**0.10/0.22**	**0.11/0.22**	**0.10/0.22**	0.22/0.32	0.15/0.30	0.18/0.29
R852	50%	0.05/0.11	**0.05/0.10**	**0.05/0.10**	0.06/0.10	0.06/0.11	0.06/0.10
GLO-M	95%	**0.12/0.21**	**0.12/0.20**	**0.12/0.21**	0.14/0.25	0.13/0.28	0.13/0.24
R859	50%	**0.05/0.09**	**0.05/0.09**	**0.05/0.09**	0.06/0.10	0.06/0.11	0.06/0.11
GLO-M+	95%	**0.11/0.20**	**0.11/0.21**	**0.11/0.20**	0.12/0.23	0.12/0.23	0.13/0.25
R802	50%	0.09/0.12	0.08/0.11	0.08/0.11	**0.08/0.10**	**0.08/0.10**	0.09/0.11
GLO-K	95%	0.38/0.50	0.39/0.47	0.39/0.47	**0.37/0.36**	**0.37/0.39**	**0.39/0.33**
C208	50%	**0.06/0.08**	**0.06/0.08**	**0.05/0.08**	0.07/0.10	**0.06/0.09**	**0.05/0.09**
BDS-3 SECM	95%	0.44/0.33	0.41/0.33	0.27/0.31	**0.11/0.22**	**0.11/0.21**	**0.13/0.21**
C206	50%	**0.08/0.11**	**0.07/0.11**	**0.07/0.11**	**0.07/0.11**	**0.07/0.10**	**0.07/0.10**
BDS-3 CAST	95%	**0.15/0.23**	**0.14/0.24**	**0.16/0.24**	0.18/0.26	0.16/0.27	**0.15/0.23**
J002	50%	0.16/0.18	**0.11/0.16**	**0.12/0.15**	0.50/0.52	0.21/0.20	0.21/0.20
QZSS-IGSO	95%	0.32/0.38	**0.27/0.24**	**0.27/0.23**	1.41/1.36	0.47/0.46	0.47/0.46

in most cases within one/two centimeters. Of these, E5 and E7 for GLONASS-K and E7 and E9 for BDS-3 SECM appear to be slightly better.

For the satellites in the GLONASS-M and GLONASS-M+ groups, the main conclusions from the long-term analyses were confirmed. In this case, the impact of the box-wing model on the prediction quality is also visible. For both groups, the differences between the various hybrid solutions are almost invisible. The differences between the individual hybrid solutions as well as those without the ECOM2 are significantly smaller than for the long-term prediction.

For the BDS-3 CAST and QZSS satellite groups, the results agree with the long-term analyses. For QZSS, the lowest median position errors were obtained for solutions B_E7 and B_E9 for each period interval of the 1st day of prediction. The results of the short-term analysis for BDS-3 CAST indicate that the box-wing model has no significant impact on

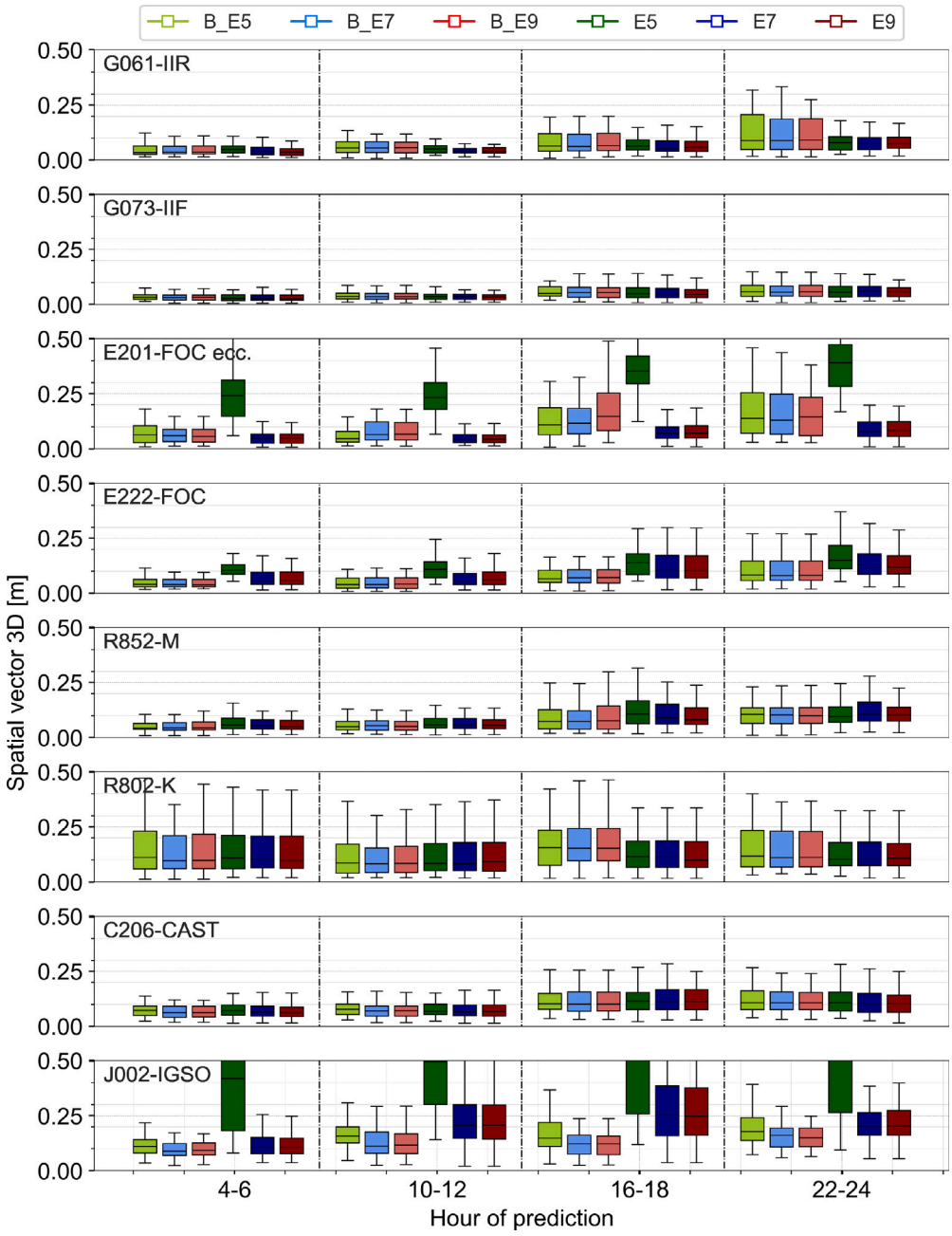

Fig. 7. Quality degradation of the first 24 h of prediction for individual satellites from the groups. The distinction was made based on individual SRP modeling solutions.

this group of satellites. The median position error values are almost the same for each solution, therefore it is not possible to select only one as the most suitable.

In summary, the results for the best strategies and all satellite groups after 12 and 24 h of prediction are as follows. For the groups of satellites for which ECOM2 is advantageous, the 95th percentile of the prediction error is 0.06/0.09, 0.08/0.14, 0.09/0.14, 0.11/0.20, 0.11/0.21, and 0.37/0.39 m for the GPS-IIF, GPS-IIR, GPS IIR-M, Galileo FOC ecc., BDS-3 SECM and GLONASS-K groups, respectively. On the other hand, there are groups for which the orbit predictions in the hybrid solution are superior. These are GPS-III, Galileo FOC, GLONASS-M+/M, BDS-3 CAST, Galileo IOV, and QZSS with 95th percentile prediction errors of 0.08/0.15, 0.10/0.22, 0.11/0.20, 0.12/0.20, 0.14/0.24, 0.16/0.28 and 0.27/0.23 m, respectively.

3.1.3. Impact of incorporating pseudo-stochastic parameters

Four additional test cases are verified to evaluate whether the introduction of pseudo-stochastic parameters improves prediction quality. The pseudo-stochastic orbit parameters are introduced in radial, along-track, and cross-track directions, at intervals of every 6 and 12 h. The 7-parameter ECOM2 with and without box-wing solutions are used as a reference for this analysis.

The analysis indicates that for all the groups of satellites of the GPS, Galileo, GLONASS, BDS-3, and QZSS constellations, the introduction of pseudo-stochastic parameters deteriorates the prediction quality (see Table 7). For the 4th day of the solution, the differences reach from several meters for GPS, Galileo, GLONASS, and BDS-3 satellites to even tens of meters for QZSS satellites. In general, pseudo-stochastic parameters introduced over a long interval reach lower median position

Table 7
Median (50%) and 95th percentile (95%) values for each processing strategy and satellite for the 4th day of prediction. SP_6h and SP_12h indicate two options with the introduction of pseudo-stochastic orbit parameters based on an interval of 6 and 12 h in the along-track, cross-track, and radial directions.

Satellite	[m]	E7	E7 SP_6h	E7 SP_12h	B_E7	B_E7 SP_6h	B_E7 SP_12h
G061	50%	0.42	3.55	3.55	1.03	7.35	4.83
GPS-IIR	95%	1.38	16.02	14.21	3.86	25.75	18.49
G050	50%	0.42	6.57	5.95	0.44	7.50	5.87
GPS-IIR-M	95%	1.50	17.03	16.90	1.23	16.95	17.17
G073	50%	0.32	5.32	5.27	0.39	6.48	5.64
GPS-IIF	95%	0.93	14.10	13.90	1.57	14.10	13.90
G077	50%	0.58	5.85	6.08	0.55	6.39	5.82
GPS-III	95%	1.95	16.27	14.59	2.06	20.54	19.58
E103	50%	1.29	5.52	3.03	0.52	5.76	1.92
GAL-IOV	95%	3.03	16.64	8.73	1.64	18.07	7.03
E201	50%	0.62	4.84	4.06	0.94	4.04	3.34
GAL-FOC ecc.	95%	2.24	18.37	15.27	3.88	18.22	10.97
E222	50%	0.71	3.33	2.30	0.52	3.62	2.07
GAL-FOC	95%	1.89	14.74	7.97	1.71	12.98	7.67
R852	50%	0.71	5.75	4.93	0.58	6.10	5.22
GLO-M	95%	3.29	18.64	18.27	2.25	23.81	16.05
R859	50%	0.86	5.21	4.83	0.74	6.99	5.71
GLO-M+	95%	2.84	18.23	16.97	2.31	20.87	17.97
C208	50%	0.53	2.54	2.78	0.59	3.00	2.97
BDS-3 SECM	95%	1.38	8.51	8.25	2.28	9.59	9.12
C206	50%	0.61	5.48	4.14	0.61	5.62	4.04
BDS-3 CAST	95%	1.91	17.10	11.61	1.88	17.35	12.14
J002	50%	1.42	17.97	17.94	0.71	17.18	17.88
QZSS-IGSO	95%	4.49	37.51	36.14	2.32	37.08	34.51

errors compared to those of 6 h. Exceptions are the BDS-3 SECM and QZSS IGSO satellite groups.

3.2. Analysis of signal-in-space range error for navigation

The orbital component of SISRE is computed to assess the quality of the short-term orbit prediction solutions provided, which is reflected in the user's positioning accuracy. For this purpose, Eq. (2) and GNSS-dependent SISRE weights factors estimated by Montenbruck et al. [43] are used. The SISRE coefficients depend mainly on the orbit altitude of the particular navigation satellites.

Fig. 8 shows the SISRE values grouped by each of the navigation satellite groups analyzed and decomposed into the total orbit error, as well as the values reduced to the effect of the radial component only. To calculate the orbital SISRE (Eq. (2)), we use the 95th percentile position errors throughout the analysis period from the 22–24 h period, and the best solution indicated in Table 6. The SISRE values can be decomposed into the radial and cross-track/along-track components separately. The component responsible for the clock was not the subject of the analysis.

GPS-IIF is the group of satellites with the lowest SISRE values of all the analyzed satellites at the level of 1.3 cm. Similar results were obtained for Galileo-FOC, GPS-IIR, GPS-IIR-M, and GLONASS-M satellites, with SISRE not exceeding 2.0 cm. Another range of values for the total orbital SISRE error, around 2.5–3 cm, was reached for groups of satellites: Galileo-IOV, Galileo-FOC ecc., GPS-III, GLONASS-M+, and BDS-3 SECM. Compared to Kazmierski et al. [44], using the accurate orbit predictions for GLONASS may be a better choice than the real-time orbits. The results for GLONASS-K are about two times worse than those for Galileo FOC and GLONASS-M, reaching about 4 cm of the orbital part of SISRE. For the BDS-3 CAST and QZSS IGSO groups, the total SISRE values are the highest, at over 4 and 5 cm, respectively.

Despite the relatively small weighting factor of the along-track and cross-track components when computing SISRE, the fast degradation of the orbit prediction for the along-track component causes a high contribution to the total SISRE. The along-track and cross-track components constitute about 75, 65, 55, 52, and 50% of the total SISRE value for GLONASS-M, GPS-IIF, Galileo FOC, GPS-IIR, and GLONASS-M+, respectively. For the remaining groups, the impact is no less than 45%.

4. Conclusions

The study investigated the quality of short- and long-term orbit predictions for GPS, Galileo, GLONASS, BDS-3 MEO, and QZSS IGSO satellites. The long-term, multi-day orbit predictions facilitate GNSS satellite tracking by laser stations. In the short time scale of up to 24 h, the near-real-time and real-time GNSS applications are of primary interest.

As a result of the research, the quality of orbit prediction for navigation satellites has been verified, and an attempt has been made to identify the optimal prediction strategy for each group of satellites.

Concerning the fit of the initial orbital arc, the results show that fitting a 2-day orbital arc is the optimal method for all the satellite groups for the best quality of orbit predictions. Regarding the SRP modeling, there is no universal optimal method for all satellites. The characteristics of each group in terms of satellite construction, optical parameters, and orbit geometry cause different approaches to be considered best for each group of the satellite. In Table 8, for several groups of satellites, more than one optimal solution has been indicated because the results obtained were at a similar level of quality. Firstly, using only constant terms of the ECOM2 model (E3 and B_E3) leads to the worst results. Secondly, there are no significant differences between solutions E5, E7, and E9 and B_E5, B_E7, and B_E9. That means that adding extra periodic ECOM2 parameters has no significant impact on the quality of the prediction even after the 4th day of the solution. The only exception is the Galileo FOC ecc. satellites, where the best quality predictions for the E7 and E9 solutions are approximately better by 1.6 m than the solution based on 5 ECOM2 parameters on the 4th day of prediction. There is a benefit of using the box-wing model for the systems, which offer access to the official detailed metadata provided by the system providers, i.e., the European GNSS Agency (GSA) for Galileo or the Japan Aerospace Exploration Agency (JAXA) for QZSS. The impact of using approximated, "best guess", or simplified satellite surface parameters for a priori orbit models is minor. This group includes GPS, BDS-3, and GLONASS satellites. Therefore, the solution should be properly selected for a specific group of satellites to properly minimize the impact of direct SRP on the quality of the orbit prediction solution for navigation satellites. Last but not least, the analysis indicates that the introduction of pseudo-stochastic parameters deteriorates the prediction quality for all the satellite groups.

5. Discussion

There are a number of issues not addressed in this study that could be explored in further research, or that should be discussed to gain a better insight into the usefulness of the findings.

In this study, the box-wing model was based on either the official metadata for the Galileo, BDS-3, and QZSS satellites or the adjusted box-wing models.[4] The official metadata are not the only source of information on BDS-3 optical properties and surfaces, as these parameters have been calibrated, e.g. by Duan et al. [45]. Using the latter could improve the solutions for the BDS-3 satellites.

The orbit prediction quality of all navigation satellites reaches a satisfactory level for the needs of SLR stations even on the 9th day of prediction. Almost every SLR station has different technology and specifications, including different detectors with different laser pulse

[4] http://acc.igs.org/repro3/PROPBOXW.f.

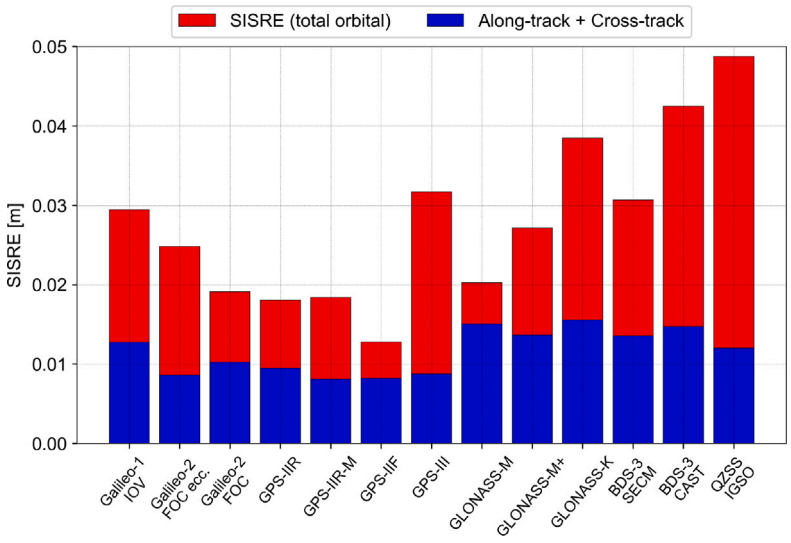

Fig. 8. Decomposition of the orbital SISRE values into sub-components based on the 95th percentile position errors after 24 h indicated in Table 6.

Table 8
The best solutions for orbit predictions using different modeling of the SRP for individual representative satellites from the groups for the 1st and 4th day of prediction (median and 95th percentile position error of the 3D spatial vector).

Type	Satellite	Median position error/95th percentile [m]			Best solutions for modeling
		1st day	4th day	9th day	the impact of SRP
GPS-IIR	G061	0.08/0.14	0.39/1.38	2.38/7.36	**E5/E7/E9**
GPS-IIR-M	G050	0.06/0.14	0.40/1.21	2.18/5.62	B_5/B_7/B_9/E5/E7/E9
GPS-IIF	G073	0.06/0.09	0.32/0.93	1.68/4.52	**E5/E7/E9**
GPS-III	G077	0.06/0.15	0.50/1.65	3.68/10.52	B_5/B_7/B_9/E5/E7/**E9**
Galileo-1 IOV	E103	0.12/0.28	0.51/1.64	2.72/8.27	**B_5**/B_7/B_9
Galileo-2 FOC (ecc. orbit)	E201	0.07/0.20	0.62/2.24	4.27/14.84	**E7**/E9
Galileo-2 FOC	E222	0.08/0.22	0.51/1.71	2.39/9.69	**B_5**/B_7/B_9
GLONASS-M	R852	0.10/0.20	0.58/2.19	3.73/11.30	B_5/B_7/**B_9**
GLONASS-M+	R859	0.08/0.20	0.73/2.24	6.42/15.73	**B_5**/B_7/B_9
GLONASS-K	R802	0.10/0.33	0.70/2.68	3.79/17.58	**E5**/E7
BDS-3 SECM	C208	0.08/0.21	0.52/1.36	2.82/8.38	**E5**/E7
BDS-3 CAST	C206	0.10/0.23	0.58/1.80	3.02/9.39	**B_5**/B_7/B_9/E5/E7/E9
QZSS IGSO	J002	0.15/0.23	0.71/2.28	2.96/7.78	B_5/**B_7/B_9**

widths or laser repetition rates. With respect to SLR tracking of GNSS satellites, the most important parameters, especially for the along-track component, are the maximum divergence of the laser beam and the range of the laser gate opening. To obtain a sufficient number of return laser pulses, it is necessary to ensure the highest possible energy concentration. Due to the above-mentioned discrepancies and the wide range of objects tracked by the laser stations, it is not possible to clearly define the required accuracy for the entire network of ILRS stations, however, the magnitude of accuracy at the level of a few meters is valid in all cases. The goal of improving prediction quality for ILRS is to increase the automation and operational speed of laser stations, especially given the ever-increasing number of satellites supported by the ILRS. Currently, laser observations are performed to 82 navigation satellites of five different satellite systems (28 Galileo, 21 GLONASS, 22 BeiDou-3, 6 IRNSS, and 5 QZSS).[5] The main problem is a large along-track offset of the satellite, the so-called time biases, which increases the target acquisition time and thus the quality and performance of the entire ILRS station network. Furthermore, the accuracy of the predictions not only impacts the time that it will take the SLR station to track the satellite but also whether such a measurement can be made at all [7,46].

In terms of the needs of real-time and near real-time users, the better orbit leads to better products, i.e., positions or zenith total delay estimates to support numerical weather prediction. In this respect, orbit predictions compete with three different types of products that can be used by real-time users: (1) broadcast message data, (2) broadcast message data corrected with real-time corrections, and (3) predicted part of ultra-rapid products. It should be noted that when discussing the usability of orbit prediction for real-time positioning, the clock error plays a key role. As shown in Kazmierski et al. [47], clock prediction can degrade the total SISRE by 10% or even 800% for Galileo FOC and GLONASS-M, respectively, depending on the stability and quality of the satellite clocks. Assessing the quality of satellite clock predictions is beyond the scope of this study. However, when providing satellite orbit and clock predictions to real-time users, the optimized orbit modeling strategy outlined in this study should be applied to achieve the best results.

[5] https://edc.dgfi.tum.de/en/satellites/.

Finally, it is necessary to discuss the impact of predicted Earth Rotation Parameters (ERP) on the quality of navigation satellite orbit predictions.

Firstly, the impact of the ERP prediction error depends directly on the orbital altitude. Therefore, the largest error is for Galileo satellites (altitude around 23 200 km) and decreases with altitude, followed by BDS-3 (21 500 km), GPS (20 200 km), and GLONASS (19 130 km). In addition to the effect of orbital altitude, the geometry of the Earth satellite also plays an important role, which is reflected in the temporal variation of the magnitude of the orbit prediction error resulting from the ERP error. Every 7 days, IERS publishes Bulletin A, which consists of the predicted ERPs for one year ahead. When using Bulletin A ERP instead of the final IERS C04, the differences in orbit error after one day reach 0.15, 0.17, 0.19, and 0.29 m for GLONASS, GPS, BDS-3, and Galileo respectively. On the 9th day, the error increases to about 4.5, 4.8, 5.0, and 5.6 m for GLONASS, GPS, BDS-3, and Galileo respectively. The orbit errors due to ERP prediction errors mainly affect the along-track component. The impact of the ERP error on the radial component is limited, reaching 0.03 and 0.3 m for the 1st and 9th day of prediction, respectively, accounting for about 5% of the total error.

It should be noted that although the IERS Bulletin A is the most widely used by users, it is not the only ERP forecast series available. The topic of improving ERP predictions is currently being studied by various groups as part of the 2nd Earth Orientation Parameters Prediction Comparison Campaign. According to recent reports, the quality of ERP predictions can be significantly improved compared to IERS Bulletin A [48]. However, we do not have information on which of these ERP forecast series are operationally provided by the responsible Analysis Centers (AC). Clearly, an improvement in the quality of the ERP forecast will lead to an improvement in the quality of the orbit forecast, but this will require either a change in the IERS Bulletin A processing strategy or the operational availability of other AC products. This issue should be further investigated in future studies. The result of this study focuses on the orbit modeling part, while the use of the predicted ERPs would introduce an additional time-varying source of error.

Declaration of competing interest

The authors declare that they have no known competing financial interests or personal relationships that could have appeared to influence the work reported in this paper.

Acknowledgments

This study was supported by the National Science Center, Poland (NCN), grant No. UMO-2021/42/E/ST10/00020. The APC is financed by Wrocław University of Environmental and Life Sciences (UPWr). We want to acknowledge the IGS MGEX for providing the multi-GNSS products. Furthermore, we extend our acknowledgments to the GSA, CSNO — Test and Assessment Research Center (TARC), and Cabinet Office (CAO) of the Government of Japan for providing publicly available information about satellite metadata.

References

[1] O. Montenbruck, Space applications, in: P.J. Teunissen, O. Montenbruck (Eds.), Springer Handbook of Global Navigation Satellite Systems, in: Springer Handbooks, Springer International Publishing, Cham, 2017, pp. 933–964, http://dx.doi.org/10.1007/978-3-319-42928-1_32.

[2] Y.J. Heo, J. Cho, M.B. Heo, Improving prediction accuracy of GPS satellite clocks with periodic variation behaviour, Meas. Sci. Technol. 21 (7) (2010) http://dx.doi.org/10.1088/0957-0233/21/7/073001.

[3] T.A. Springer, U. Hugentobler, IGS ultra rapid products for (near-) real-time applications, Phys. Chem. Earth A: Solid Earth Geod. 26 (6) (2001) 623–628, http://dx.doi.org/10.1016/S1464-1895(01)00111-9.

[4] T. Hadas, J. Bosy, IGS RTS precise orbits and clocks verification and quality degradation over time, GPS Solut. 19 (1) (2015) 93–105, http://dx.doi.org/10.1007/s10291-014-0369-5.

[5] G. Johnston, A. Riddell, G. Hausler, The international GNSS service, in: P.J. Teunissen, O. Montenbruck (Eds.), Springer Handbook of Global Navigation Satellite Systems, in: Springer Handbooks, Springer International Publishing, Cham, 2017, pp. 967–982, http://dx.doi.org/10.1007/978-3-319-42928-1_33.

[6] X. Li, Y. Yuan, Y. Zhu, W. Jiao, L. Bian, X. Li, K. Zhang, Improving BDS-3 precise orbit determination for medium earth orbit satellites, GPS Solut. 24 (2) (2020) 53, http://dx.doi.org/10.1007/s10291-020-0967-3.

[7] M.R. Pearlman, C.E. Noll, E.C. Pavlis, F.G. Lemoine, L. Combrink, J.J. Degnan, G. Kirchner, U. Schreiber, The ILRS: approaching 20 years and planning for the future, J. Geod. 93 (11) (2019) 2161–2180, http://dx.doi.org/10.1007/s00190-019-01241-1.

[8] J. Najder, K. Sośnica, Quality of orbit predictions for satellites tracked by SLR stations, Remote Sens. 13 (7) (2021) 1377, http://dx.doi.org/10.3390/rs13071377.

[9] O. Montenbruck, P. Steigenberger, M. Aicher, A long-term broadcast ephemeris model for extended operation of GNSS satellites, Navigation 68 (1) (2021) 199–215, http://dx.doi.org/10.1002/navi.404.

[10] A. Pukkila, J. Ala-Luhtala, R. Piché, S. Ali-Löytty, GNSS orbit prediction with enhanced force model, in: 2015 International Conference on Localization and GNSS (ICL-GNSS), 2015, pp. 1–6, http://dx.doi.org/10.1109/ICL-GNSS.2015.7217145.

[11] J. Qiao, G. Xu, W. Liu, P. Fang, W. Chen, Comparison of Beidou autonomous navigation performance using the SRP model and onboard accelerometers, Acta Astronaut. 173 (2020) 183–194, http://dx.doi.org/10.1016/j.actaastro.2020.04.018.

[12] K.K. Choi, J. Ray, J. Griffiths, T.-S. Bae, Evaluation of GPS orbit prediction strategies for the IGS ultra-rapid products, GPS Solut. 17 (3) (2013) 403–412, http://dx.doi.org/10.1007/s10291-012-0288-2.

[13] T. Geng, P. Zhang, W. Wang, X. Xie, Comparison of ultra-rapid orbit prediction strategies for GPS, GLONASS, Galileo and BeiDou, Sensors 18 (2) (2018) 477, http://dx.doi.org/10.3390/s18020477.

[14] O. Montenbruck, P. Steigenberger, L. Prange, Z. Deng, Q. Zhao, F. Perosanz, I. Romero, C. Noll, A. Stürze, G. Weber, R. Schmid, K. MacLeod, S. Schaer, The multi-GNSS experiment (MGEX) of the international GNSS service (IGS) – achievements, prospects and challenges, Adv. Space Res. 59 (7) (2017) 1671–1697, http://dx.doi.org/10.1016/j.asr.2017.01.011.

[15] B. Duan, U. Hugentobler, J. Chen, I. Selmke, J. Wang, Prediction versus real-time orbit determination for GNSS satellites, GPS Solut. 23 (2) (2019) 39, http://dx.doi.org/10.1007/s10291-019-0834-2.

[16] G. Beutler, E. Brockmann, W. Gurtner, U. Hugentobler, L. Mervart, M. Rothacher, A. Verdun, Extended orbit modeling techniques at the CODE processing center of the international GPS service for geodynamics (IGS): theory and initial results, Manuscr. Geod. 19 (6) (1994) 367–386, URL: https://ui.adsabs.harvard.edu/abs/1994MGeo...19..367B.

[17] T. Springer, Modeling and Validating Orbits and Clocks using the Global Positioning System, Schweizerische Geodätische Kommission, Zürich, Schweiz, 2000, URL: http://www.gbv.de/dms/goettingen/352089008.pdf.

[18] D. Arnold, M. Meindl, G. Beutler, R. Dach, S. Schaer, S. Lutz, L. Prange, K. Sośnica, L. Mervart, A. Jäggi, CODE's new solar radiation pressure model for GNSS orbit determination, J. Geod. 89 (8) (2015) 775–791, http://dx.doi.org/10.1007/s00190-015-0814-4.

[19] X. Li, Y. Yuan, J. Huang, Y. Zhu, J. Wu, Y. Xiong, X. Li, K. Zhang, Galileo and QZSS precise orbit and clock determination using new satellite metadata, J. Geod. 93 (8) (2019) 1123–1136, http://dx.doi.org/10.1007/s00190-019-01230-4.

[20] G. Bury, K. Sośnica, R. Zajdel, D. Strugarek, Toward the 1-cm Galileo orbits: challenges in modeling of perturbing forces, J. Geod. 94 (2) (2020) 16, http://dx.doi.org/10.1007/s00190-020-01342-2.

[21] O. Montenbruck, P. Steigenberger, A. Hauschild, Multi-GNSS signal-in-space range error assessment – methodology and results, Adv. Space Res. 61 (12) (2018) 3020–3038, http://dx.doi.org/10.1016/j.asr.2018.03.041.

[22] R. Dach, F. Andritsch, D. Arnold, S. Bertone, P. Fridez, A. Jäggi, Y. Jean, A. Maier, L. Mervart, U. Meyer, E. Orliac, E. Geist, L. Prange, S. Scaramuzza, S. Schaer, D. Sidorov, A. Susnik, A. Villiger, P. Walser, D. Thaller, Bernese GNSS Software Version 5.2, Astronomical Institute, University of Bern, Bern, 2015, http://dx.doi.org/10.7892/boris.72297.

[23] L. Prange, A. Villiger, D. Sidorov, S. Schaer, G. Beutler, R. Dach, A. Jäggi, Overview of CODE's MGEX solution with the focus on galileo, Adv. Space Res. 66 (12) (2020) 2786–2798, http://dx.doi.org/10.1016/j.asr.2020.04.038.

[24] L. Prange, D. Arnold, R. Dach, M.S. Kalarus, S. Schaer, P. Stebler, A. Villiger, A. Jäggi, CODE Product Series for the IGS-MGEX Project, Astronomical Institute, University of Bern, 2020, [Dataset]. URL: http://www.aiub.unibe.ch/download/CODE_MGEX.

[25] C.J. Rodriguez-Solano, U. Hugentobler, P. Steigenberger, M. Bloßfeld, M. Fritsche, Reducing the draconitic errors in GNSS geodetic products, J. Geod. 88 (6) (2014) 559–574, http://dx.doi.org/10.1007/s00190-014-0704-1.

[26] R.B. Langley, P.J. Teunissen, O. Montenbruck, Introduction to GNSS, in: P.J. Teunissen, O. Montenbruck (Eds.), Springer Handbook of Global Navigation Satellite Systems, in: Springer Handbooks, Springer International Publishing, Cham, 2017, pp. 3–23, http://dx.doi.org/10.1007/978-3-319-42928-1_1.

[27] G. Petit, B. Luzum, IERS Conventions (2010), Technical Report, IERS Technical Note; No. 36, Verlag des Bundesamts für Kartographie und Geodäsie, Frankfurt am Main, 2010, URL: https://www.iers.org/IERS/EN/Publications/TechnicalNotes/tn36.html.

[28] P. Rebischung, R. Schmid, IGS14/igs14.atx: a new framework for the IGS products, in: AGU Fall Meeting, 2016, URL: https://mediatum.ub.tum.de/doc/1341338/file.pdf.

[29] F. Lyard, F. Lefevre, T. Letellier, O. Francis, Modelling the global ocean tides: modern insights from FES2004, Ocean Dyn. 56 (5) (2006) 394–415, http://dx.doi.org/10.1007/s10236-006-0086-x.

[30] C. Bizouard, S. Lambert, C. Gattano, O. Becker, J.-Y. Richard, The IERS EOP 14c04 solution for earth orientation parameters consistent with ITRF 2014, J. Geod. 93 (5) (2019) 621–633, http://dx.doi.org/10.1007/s00190-018-1186-3.

[31] N.K. Pavlis, S.A. Holmes, S.C. Kenyon, J.K. Factor, The development and evaluation of the earth gravitational model 2008 (EGM2008), J. Geophysi. Res.: Solid Earth 117 (B4) (2012) http://dx.doi.org/10.1029/2011JB008916.

[32] P.M. Mathews, T.A. Herring, B.A. Buffett, Modeling of nutation and precession: New nutation series for nonrigid earth and insights into the earth's interior, J. Geophys. Res.: Solid Earth 107 (B4) (2002) ETG 3–1–ETG 3–26, http://dx.doi.org/10.1029/2001JB000390.

[33] P.M. Mathews, P. Bretagnon, Polar motions equivalent to high frequency nutations for a nonrigid earth with anelastic mantle, Astron. Astrophys. 400 (3) (2003) 1113–1128, http://dx.doi.org/10.1051/0004-6361:20021795.

[34] D. Ineichen, G. Beutler, U. Hugentobler, Sensitivity of GPS and GLONASS orbits with respect to resonant geopotential parameters, J. Geod. 77 (7) (2003) 478–486, http://dx.doi.org/10.1007/s00190-003-0348-z.

[35] U. Hugentobler, D. Ineichen, G. Beutler, GPS satellites: Radiation pressure, attitude and resonance, Adv. Space Res. 31 (8) (2003) 1917–1926, http://dx.doi.org/10.1016/S0273-1177(03)00174-1.

[36] G. Beutler, L. Mervart, A. Verdun, Methods of Celestial Mechanics: Volume II: Application To Planetary System, Geodynamics and Satellite Geodesy, 2005th ed., Springer Berlin, Heidelberg, Berlin ; New York, 2004, http://dx.doi.org/10.1007/b137725.

[37] G. Bury, R. Zajdel, K. Sośnica, Accounting for perturbing forces acting on galileo using a box-wing model, GPS Solut. 23 (3) (2019) 74, http://dx.doi.org/10.1007/s10291-019-0860-0.

[38] R. Zajdel, K. Sośnica, G. Bury, Geocenter coordinates derived from multi-GNSS: a look into the role of solar radiation pressure modeling, GPS Solut. 25 (1) (2020) 1, http://dx.doi.org/10.1007/s10291-020-01037-3.

[39] R. Zajdel, P. Steigenberger, O. Montenbruck, On the potential contribution of BeiDou-3 to the realization of the terrestrial reference frame scale, GPS Solut. 26 (4) (2022) 109, http://dx.doi.org/10.1007/s10291-022-01298-0.

[40] A. Jäggi, U. Hugentobler, G. Beutler, Pseudo-stochastic orbit modeling techniques for low-earth orbiters, J. Geod. 80 (1) (2006) 47–60, http://dx.doi.org/10.1007/s00190-006-0029-9.

[41] C.J. Rodriguez-Solano, U. Hugentobler, P. Steigenberger, S. Lutz, Impact of earth radiation pressure on GPS position estimates, J. Geod. 86 (5) (2012) 309–317, http://dx.doi.org/10.1007/s00190-011-0517-4.

[42] K. Sośnica, L. Prange, K. Kaźmierski, G. Bury, M. Drożdżewski, R. Zajdel, T. Hadas, Validation of Galileo orbits using SLR with a focus on satellites launched into incorrect orbital planes, J. Geod. 92 (2) (2018) 131–148, http://dx.doi.org/10.1007/s00190-017-1050-x.

[43] O. Montenbruck, P. Steigenberger, A. Hauschild, Broadcast versus precise ephemerides: a multi-GNSS perspective, GPS Solut. 19 (2) (2015) 321–333, http://dx.doi.org/10.1007/s10291-014-0390-8.

[44] K. Kazmierski, R. Zajdel, K. Sośnica, Evolution of orbit and clock quality for real-time multi-GNSS solutions, GPS Solut. 24 (4) (2020) 111, http://dx.doi.org/10.1007/s10291-020-01026-6.

[45] B. Duan, U. Hugentobler, I. Selmke, S. Marz, M. Killian, M. Rott, BeiDou satellite radiation force models for precise orbit determination and geodetic applications, IEEE Trans. Aerosp. Electron. Syst. 58 (4) (2022) 2823–2836, http://dx.doi.org/10.1109/TAES.2021.3140018.

[46] S. Bauer, J. Steinborn, Time bias service: analysis and monitoring of satellite orbit prediction quality, J. Geod. 93 (11) (2019) 2367–2377, http://dx.doi.org/10.1007/s00190-019-01304-3.

[47] K. Kazmierski, K. Sośnica, T. Hadas, R. Zajdel, Quality assessment of real-time products, in: Scientific and Fundamental Aspects of GNSS, 8th International Colloquium, Sofia, Bulgaria, 2022.

[48] J. Nastula, H. Dobslaw, J. Śliwińska, T. Kur, M. Wińska, A. Partyka, Summary of the second earth orientation parameters prediction comparison campaign (2nd EOP pcc), in: 2nd EOP PCC Workshop No. 2, 1 – 3 March 2023, Alicante, Spain & Online, 2023, URL: https://drive.cbk.waw.pl/apps/onlyoffice/s/N44dgAz5sqtyeAw?fileId=5208677.